



HAL
open science

Comparison of methods for the fabrication and the characterization of polymer self-assemblies

M. Dionzou, A. Morère, Clément Roux, Barbara Lonetti, Jean-Daniel Marty, Christophe Mingotaud, Pierre Joseph, D. Goudouneche, B. Payre, M. Leonetti, et al.

► To cite this version:

M. Dionzou, A. Morère, Clément Roux, Barbara Lonetti, Jean-Daniel Marty, et al.. Comparison of methods for the fabrication and the characterization of polymer self-assemblies: what are the important parameters?. *Soft Matter*, 2016, 12 (7), pp.2166-2176. 10.1039/c5sm01863c . hal-01314955

HAL Id: hal-01314955

<https://hal.science/hal-01314955>

Submitted on 20 Feb 2023

HAL is a multi-disciplinary open access archive for the deposit and dissemination of scientific research documents, whether they are published or not. The documents may come from teaching and research institutions in France or abroad, or from public or private research centers.

L'archive ouverte pluridisciplinaire **HAL**, est destinée au dépôt et à la diffusion de documents scientifiques de niveau recherche, publiés ou non, émanant des établissements d'enseignement et de recherche français ou étrangers, des laboratoires publics ou privés.



Distributed under a Creative Commons Attribution - NonCommercial 4.0 International License



Cite this: *Soft Matter*, 2016, 12, 2166

Comparison of methods for the fabrication and the characterization of polymer self-assemblies: what are the important parameters?†

M. Dionzou,^a A. Morère,^a C. Roux,^{ab} B. Lonetti,^a J.-D. Marty,^a C. Mingotaud,^a P. Joseph,^{bc} D. Goudounèche,^d B. Payré,^d M. Léonetti^e and A.-F. Mingotaud^{*a}

The ability to self-assemble was evaluated for a large variety of amphiphilic block copolymers, including poly(ethyleneoxide-*b*- ϵ -caprolactone), poly(ethyleneoxide-*b*-D,L-lactide), poly(ethyleneoxide-*b*-styrene), poly(ethyleneoxide-*b*-butadiene) and poly(ethyleneoxide-*b*-methylmethacrylate). Different methods of formation are discussed, such as cosolvent addition, film hydration or electroformation. The influence of experimental parameters and macromolecular structures on the size and morphology of the final self-assembled structures is investigated and critically compared with the literature. The same process is carried out regarding the characterization of these structures. This analysis demonstrates the great care that should be taken when dealing with such polymeric assemblies. If the morphology of such assemblies can be predicted to some extent by macromolecular parameters like the hydrophilic/hydrophobic balance, those parameters cannot be considered as universal. In addition, external experimental parameters (methods of preparation, use of co-solvent, ...) appeared as critical key parameters to obtain a good control over the final structure of such objects, which are very often not at thermodynamic equilibrium but kinetically frozen. A principal component analysis is also proposed, in order to examine the important parameters for forming the self-assemblies. Here again, the hydrophilic/hydrophobic fraction is identified as an important parameter.

Received 27th July 2015,
Accepted 23rd December 2015

DOI: 10.1039/c5sm01863c

www.rsc.org/softmatter

Introduction

Precision polymer engineering has yielded a plethora of newly synthesized copolymers with controlled composition, chain length, chemical functions and morphologies. In parallel, polymer self-assemblies in aqueous solutions have shown increasing potential, in particular, in biomedical applications such as drug delivery. This was stimulated by the development of encapsulated drugs using pegylated liposomes, which showed improved biodistribution and limited side effects.^{1–3} Kataoka's team in Japan has made an

enormous contribution to this topic, publishing *ca.* 1000 papers^{4–6} on self-assembled polymer systems. The synthesis of biocompatible amphiphilic copolymers and characterization of their self-assemblies sparked the interest of a large community and has been extensively described.^{3,6–9}

Polymer drug vectors have the advantage of being easily tunable, in contrast to regular liposomes formed by small surfactants. In addition, the average size of polymeric micelles and vesicles falls within the 15–200 nm range which is suitable for intravenous drug delivery.^{1,10} Polymeric micelles are smaller in size enabling them to penetrate narrow capillaries or disjunctions, while vesicles are able to encapsulate either hydrophilic or hydrophobic drugs.

Polymeric micelles are by far the most commonly described structures in the literature. Their structure is sometimes more complex than that of surfactant micelles (*i.e.* a pure hydrophobic core surrounded by a hydrophilic layer). Indeed, they may consist of nano-objects with a structured core, or may more accurately be described as simple polymeric nanoparticles.

Polymer vesicles have been studied for over 20 years, since the early papers of Discher and Eisenberg^{11,12} and have recently gained much interest in biomedical applications. Polymer vesicles are also known as polymersomes, by analogy with liposomes

^a Université de Toulouse, UPS/CNRS, IMRCP, 118 route de Narbonne, F-31062 Toulouse Cedex 9, France. E-mail: afmingo@chimie.ups-tlse.fr

^b CNRS, LAAS, 7 avenue du colonel Roche, F-31400 Toulouse, France

^c Université de Toulouse, LAAS, F-31400 Toulouse, France

^d Centre de Microscopie Electronique Appliquée à la Biologie, Faculté de Médecine Toulouse Rangueil, Université de Toulouse, 133, route de Narbonne, 31062 Toulouse Cedex 4, France

^e Aix-Marseille Université, CNRS, Centrale Marseille, IRPHE UMR 7342, Technopôle de Château-Gombert, 13384 Marseille Cedex 13, France

† Electronic supplementary information (ESI) available: Tabulation of all copolymers used, chemical structures, experimental details for analyses, acetonitrile cosolvent methods, TEM and optical microscopy images of nano-objects, explanation of DLS methods and discussion, hydrophilic fraction calculations, PCA analysis data, and comments on two problematic copolymers. See DOI: 10.1039/c5sm01863c

obtained from the self-assembly of lipids. The first polymers to be described as capable of vesicle formation were poly(ethyleneoxide-*b*-ethylethylene) (PEO-PEE) and poly(styrene-*b*-acrylic acid) (PS-PAA). Shortly afterwards, poly(ethyleneoxide-*b*-butadiene) (PEO-PBD) was also thoroughly assessed,^{13–17} because of its ability to self-assemble into various morphologies and sizes, up to several microns. These were the first giant polymer vesicles, which allowed single objects to be visualized and manipulated. Aspiration techniques were used to characterize the mechanical properties of these polymersomes and compare them with lipid vesicles. They showed a strong increase in bending modulus and shear viscosity¹⁸ together with lower water permeability and lateral diffusion coefficient.¹⁹

As drug release is sometimes a weakness of the polymersomes, various teams have developed stimuli-responsive systems which are able to release their content upon demand, either using temperature, pH, redox reactions or an external magnetic field.^{9,20} Numerous examples have been presented in the literature, leading to commonly repeated assertions about formation criteria. However very few studies have dealt with very different polymers of different hydrophilic fractions. Such studies are essential in order to acquire a critical understanding of the different processes involved in the formation of self-assemblies. Therefore, the work described here consists of examining various techniques for the formation of self-assemblies from a wide range of amphiphilic copolymers. The resulting objects have been characterized by dynamic light scattering and electron microscopy, the two techniques found in all papers dealing with polymer self-assemblies. The results are used to point out essential experimental parameters as well as frequently overlooked difficulties in characterization.

Materials and methods

All copolymers were bought from Polymer Source Inc. (Dorval Montréal, Canada). They were systematically characterized by ¹H NMR and Size Exclusion Chromatography (SEC) (Table S1, ESI†). Ultrapure water was obtained from an ELGA Purelab Flex system (resistivity higher than 18.2 MΩ cm) and was filtered on 0.2 μm RC filters just before use.

“Acetone cosolvent” method

20 mg of polymer were dissolved in 0.4 mL of acetone. This was added dropwise over 10–15 minutes to 5 mL of ultrapure water under stirring. The solution was left standing for two days for acetone to evaporate. The reverse addition, in which water was added to the acetone solution, was also used with the same duration for the addition. The “acetonitrile cosolvent” method was strictly identical, except that acetone was replaced by acetonitrile.

“THF/MeOH cosolvent” method

The polymer was first dissolved in 0.5 mL of a THF/MeOH 75/25 v/v solution at a concentration of 100 mg mL⁻¹. To this, 5 mL of filtered 4 wt% benzyl alcohol aqueous solution were added over 2 hours using an automatic syringe and a stirring speed of 500 rpm. THF, MeOH and benzyl alcohol were then removed

by dialysis (GE Healthcare Bio-Sciences membranes with a MWCO of 8000 g mol⁻¹).

“Meng” method

The polymer was dissolved in THF (0.1 mL, 10 mg mL⁻¹) and injected at the bottom of a 4 wt% benzyl alcohol aqueous solution (5 mL) in 2 minutes without stirring. After 10 minutes, the solution was shaken twice and dialyzed to remove the organic compounds.

“Film hydration” method

A 2 mg mL⁻¹ polymer solution in chloroform was prepared and the solvent was evaporated on a rotary evaporator to form a regular thin film which was further dried under vacuum for 4 hours. The film was then rehydrated with 5 mL of ultrapure water and heated at 60 °C for several days.

All the other methods are described in the ESI.†

Results

Self-assembly formation

Based on the existing literature, different PEO-based block copolymers were selected (Fig. 1), with hydrophilic weight fractions f_{PEO} ranging from 0.13 to 0.55 and different hydrophobic blocks, namely poly(butadiene), poly(ε-caprolactone), polylactide, polystyrene or poly(methylmethacrylate) (see Table S1, ESI† for the molecular weights). For each polymer, different methods of self-assembly formation were examined. First, a cosolvent technique was used (also called nanoprecipitation). This consists of dissolving the polymer in an organic solvent which is water miscible and mixing it with water, adding either organic solvent into water or the reverse. The chosen solvents were acetone, acetonitrile or THF/MeOH 75/25 v/v.^{21–23} A derived technique described by Meng and Feijen was also used, where the addition of a THF solution into a 4 wt% aqueous benzyl alcohol solution was performed without any stirring.²⁴

Tables 1 and 2 present the results obtained using acetone as the cosolvent, respectively by “normal” addition (acetone into water) or reverse addition (water into acetone). The self-assemblies were characterized by DLS and, in selected cases, by TEM (Fig. 2 and photographs in the ESI†). Two DLS size results are given in all following tables, designated as “DLS size int”

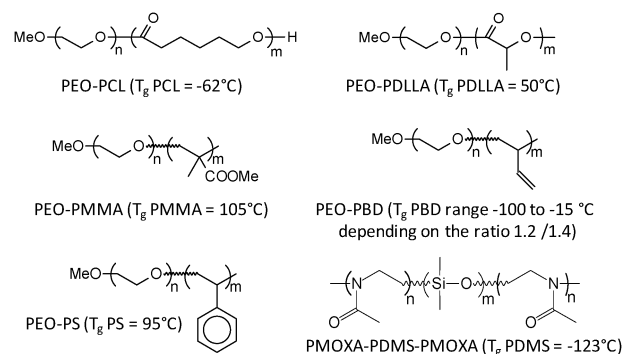


Fig. 1 Polymers used in this study.

Table 1 Results obtained from the “acetone cosolvent” method using the addition of acetone into water

Polymers	$f_{\text{PEO exp}}$	DLS size int (nm)	DLS size number (nm)	PDI	Mean size from TEM (nm)	Morphology from TEM
PEO5000-PCL33300	0.13	280	130	0.3	180 ± 80	Polymersomes/nanoparticles (NP)?
PEO2000-PCL13300	0.13	80	45	0.1	42 ± 14	Micelles/polymersomes
PEO2000-PCL8800	0.19	40	25	0.2		Micelles ^a
PEO2000-PCL6700	0.23	26/390	16	0.6	26 ± 14	Micelles
PEO2000-PCL5800	0.26	30	20	0.1		Micelles ^a
PEO5000-PCL10800	0.32	134	16	0.2		Micelles/polymersomes
PEO2000-PCL2800	0.42	20	15	0.2	14 ± 3	Micelles ^{21,23,27}
PEO5000-PCL4000	0.56	25	15	0.3	13 ± 3	Micelles ^{21,23,27}
PEO11000-PMMA66500	0.14	50	30	0.2		Micelles ^a
PEO2000-PMMA5040	0.28	84	29	0.21	11 ± 2	Micelles
PEO5000-PMMA11900	0.30	35	20	0.2		Micelles ^a
PEO5000-PMMA4100	0.55	25	15	0.2		Micelles ^a
PEO5000-PDLLA20500	0.20	175	135	0.05	29 ± 18	Polymersomes
PEO2000-PDLA5450	0.27	210	110	0.3	42 ± 26	Micelles/polymersomes/worm-like
PEO5000-PDLLA10550	0.32	190	120	0.1	29 ± 22	Polymersomes/micelles
PEO10000-PDLLA17650	0.36	70	40	0.1	23 ± 6	Micelles
PEO10000-PLLA12800	0.44	210	140	0.1	84 ± 42	Micelles/polymersomes
PEO2400-PDLLA2000	0.55	30	15	0.2		Micelles ^{21,23,27}
PEO15000-PS37300	0.29	60	35	0.4		Micelles ^a
PEO3100-PS2300	0.57	20	15	0.3	12 ± 2	Micelles ^{21,23,27}
PCL12300-PEO5000-PCL12300	0.17	670	220	0.3	250 ± 245	Polymersomes/NP?
PCL8250-PEO10000-PCL8250	0.38	160	100	0.1		Micelles/NP? ^a
PCL4400-PEO10000-PCL4400	0.53	90	50	0.1		Micelles ^a

^a No TEM performed, morphology suggested only from the DLS size.

Table 2 Results obtained from “acetone cosolvent” method using the addition of water into acetone

Polymers	$f_{\text{PEO exp}}$	DLS size int (nm)	DLS size number (nm)	PDI	Mean size from TEM (nm)	Morphology from TEM
PEO5000-PCL33300	0.13	170	130	0.3	125 ± 70	Polymersomes/NP?
PEO2000-PCL13300	0.13	55	35	0.1	47 ± 19	Micelles/NP
PEO5000-PMMA11900	0.30	25	15	0.1		Micelles ^a
PEO5000-PMMA4100	0.55	30	20	0.2		Micelles ^a
PEO2000-PDLA5450	0.27	840	450	0.2		Nanocrystals
PEO5000-PDLLA10550	0.32	300	180	0.2	49 ± 47	Polymersomes/micelles
PEO10000-PDLLA17650	0.36	130	40	0.2	23 ± 10	Micelles
PEO10000-PLLA12800	0.44	460	290	0.3		Micelles/nanocrystals
PEO15000-PS37300	0.29	55	35	0.6		Micelles ^a
PCL12300-PEO5000-PCL12300	0.17	1700	400	0.3		Polymersomes/NP?
PCL8250-PEO10000-PCL8250	0.38	210	90	0.2		Micelles ^a
PCL4400-PEO10000-PCL4400	0.53	1100/190/50	35	1.0		Micelles ^a /NP?

^a No TEM performed, morphology suggested only from the DLS size.

and “DLS size number”. DLS size int corresponds to the analysis of the DLS correlogram based on the scattered intensity, whereas the DLS size number has been corrected in order to avoid over-representing large scattering objects (a more detailed explanation is given in the ESI†). In the following tables, each time that worm-like systems have been detected (by TEM), the DLS result should be taken with great care, since the general treatment assumes an isotropic shape for the scattering objects. Fig. 2 illustrates some typical morphologies that were observed by TEM or cryo-SEM. TEM photographs for all experiments described in this manuscript are provided in the ESI.†

From a general standpoint, micelles are more readily formed for high f_{PEO} . However, discrepancies between polymer types are visible. For PEO-PCL, polymersomes (or nanoparticles noted NP) are formed at f_{PEO} as low as 0.13, while micelles were observed at higher f_{PEO} . For PEO-PDLLA, the threshold f_{PEO} for micelle formation is higher, close to 0.4. For PEO-PMMA and PEO-PS, only micelles were obtained. Triblock copolymers with high hydrophilic fractions also produce micelles. In some cases, mixtures of morphologies were observed, as well as worm-like self-assemblies.

Comparing Tables 1 and 2 shows that for most polymers changing the sequence of addition did not lead to fundamental

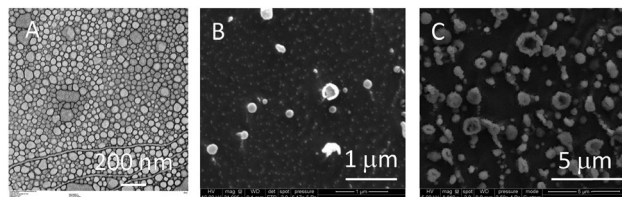


Fig. 2 (A) TEM PEO2000-PCL13300 “acetone cosolvent method” using addition of acetone into water. (B) cryo-SEM PEO5000-PCL33300 “acetone cosolvent method” using acetone addition into water. (C) Cryo-SEM PEO2000-PMMA5040 “THF/MeOH cosolvent method” using addition of water/benzyl alcohol into THF/MeOH solution.

changes in morphologies, but “reverse” addition of water into acetone generally led to slightly larger objects than the “normal” addition. However, for PEO-PDLA, PEO-PLLA and PCL-PEO-PCL polymers, the change of the addition sequence led to the appearance of nanocrystals (PEO-PDLA) or to a strong increase in size or polydispersity (PEO-PLLA and PCL-PEO-PCL). This might be because acetone addition into a large excess of water produces an instantaneous change of solvent quality for the hydrophobic block, leading to the formation of objects that are unlikely to evolve afterwards: the object formation is under kinetic control. On the other hand, the addition of water to acetone solution leads to a slow change in solvent quality, allowing the system to rearrange during the process,^{25,26} before becoming frozen at high water content.

In order to further explore the preparation processes, acetonitrile was also used as cosolvent in the formation of nano-objects (addition of acetonitrile solution into water). The results are presented in the ESI† (Table S3). This mostly led to a small decrease in the size of the nano-objects.

Table 3 presents the results obtained by slow addition of a benzyl alcohol solution to polymeric THF/MeOH solutions.²² Benzyl alcohol was used following the example of Meng²⁴ to favor larger self-assemblies. Since benzyl alcohol has a partition

coefficient $\log P$ equal to 1.1, it is soluble in water up to 4 wt% but in the presence of amphiphilic molecules such as block copolymers, partition will occur. The presence of excess benzyl alcohol in the core of the self-assemblies can be expected to lead to larger objects. Here again, for PEO-PCL, polymersomes were obtained for low hydrophilic fractions. For PEO5000-PCL33300, this method did not lead to a strong modification of the self-assemblies. However, for PEO2000-PCL13300 and PEO2000-PCL5800, a strong increase in size was observed by DLS. TEM revealed the presence of polymersomes for the former and worm-like systems for the latter (ESI†). The PEO2000-PCL6700 and PEO2000-PCL5800 cases show that even slight differences in molecular weights and hydrophilic fractions can lead to different objects. In the first case, micelles are obtained, whereas a mixture of micelles and worm-like systems is formed for the second. As already mentioned, the presence of worm-like scattering objects implies that the DLS analysis should be taken only as an indication. Samples of PEO-PMMA and PEO-PS yielded micelles, similar to when acetone was used (Table 1). However, PEO2000-PMMA5040 led to the formation of large polymersomes with a size of 550 nm. This morphology was only obtained in the presence of benzyl alcohol. The addition of pure water into THF/MeOH solution resulted in the formation of 18 nm micelles (data not shown).

The last cosolvent method used in this study was that suggested by Meng²⁴ (Table 4). Here again, benzyl alcohol was used to favor larger self-assemblies and the addition of the organic solution was performed at the bottom of the flask without any stirring. In Meng’s work, this led to large (>400 nm) polymersomes of PEO-PCL and PEO-PDLLA. In our case, large polymersomes were not obtained; the self-assemblies were similar to those obtained by the acetone addition in the case of PEO-PCL, except for PEO2000-PCL13300 for which an increase of size was noted. For PEO-PMMA and PEO-PDLLA, all assemblies were larger. Finally for the triblock copolymer, nanoparticles with undefined shapes and polymersomes were obtained.

Table 3 Results obtained by the “THF/MeOH cosolvent” method with the addition of water/benzyl alcohol into THF/MeOH solution

Polymers	$f_{\text{PEO exp}}$	DLS size int (nm)	DLS size number (nm)	PDI	Mean size from TEM (nm)	Morphology from TEM
PEO5000-PCL33300	0.13	150/4000	80	0.2		Polymersomes ^{b?}
PEO2000-PCL13300	0.13	280	230	0.1	130 ± 100	Polymersomes/micelles
PEO2000-PCL8800	0.19	210	150	0.1	41 ± 63 ^a	Micelles/polymersomes
PEO2000-PCL6700	0.23	40/370	25	0.4		Micelles ^b
PEO2000-PCL5800	0.26	190	140	0.1		Micelles, worm-like systems
PEO5000-PCL10800	0.32	50/360	35	0.3		Micelles ^b
PEO11000-PMMA66500	0.14	80	50	0.1		Micelles ^b
PEO5000-PMMA21500	0.19	50	30	0.1		Micelles ^b
PEO2000-PMMA5040	0.28	1020	550	0.2	375 ± 125	Polymersomes
PEO5000-PDLLA20500	0.20	180/70	55	0.7	37 ± 14	Micelles
PEO15000-PS37300	0.29	170	40	0.4	46 ± 11	Micelles
PEO3900-PBD6700	0.37	61	27	0.2	25 ± 8	Micelles + a few polymersomes

^a Mean population at around 30 nm with other objects up to 400 nm. ^b No TEM performed, morphology suggested only from the DLS size. For PEO2000-PCL6700 and PEO5000-PCL10800, the peak relative to the population only seen in intensity DLS analysis is small enough to assume that larger objects are only present as traces.

Table 4 Results obtained from the "Meng" method

Polymers	$f_{\text{PEO exp}}$	DLS size int (nm)	DLS size number (nm)	PDI	Morphology from TEM
PEO5000-PCL33300	0.13	270	180	0.1	Polymersomes ^a ?
PEO2000-PCL13300	0.13	320	300	0.2	Polymersomes
PEO2000-PCL8800	0.19	140/35	30	0.4	Micelles/polymersomes ^a ?
PEO2000-PCL6700	0.23	170/40	40	0.3	Micelles, worm-like micelles
PEO2000-PCL5800	0.26	50	20	0.4	Micelles ^a
PEO5000-PCL10800	0.32	100	70	0.1	Micelles or polymersomes ^a ?
PEO11000-PMMA66500	0.14	230	120	0.2	Polymersomes/NP ^a ?
PEO5000-PMMA21500	0.19	190	130	0.2	Polymersomes/NP ^a ?
PEO5000-PDLLA20500	0.20	205	130	0.1	Polymersomes
PEO5000-PDLLA10550	0.32	240	180	0.2	Micelles, polymersomes
PCL12300-PEO5000-PCL12300	0.17	570	570	0.7	Aggregates, undefined shapes
PEO3900-PBD6700	0.37	130	40	0.3	Micelles, worm-like micelles

^a No TEM performed, morphology suggested only from DLS size.

Film rehydration is another commonly used method to form giant polymersomes. In the method we used, polymersomes are indeed observed for some cases together with other morphologies (Table 5). The general trend is the formation of mixed morphologies, which is also indicated by an increase of the polydispersities measured by DLS. It is noteworthy that we decided not to examine the formation of nano-objects by film rehydration/extrusion techniques. These have been shown to reduce the size of the nano-objects formed, associated with the size of the filter pore.^{28–31} Our intent was to assess the morphologies of nano-objects "as-formed", directly after self-assembly.

Closely related to film rehydration, electroformation is another method first developed for the fabrication of giant lipid vesicles³² that can also be used for giant polymersome formation. Although this was described more than a decade ago for PEO-PBD copolymers,¹⁸ some experimental details are worth discussing. Table 6 thus presents some of the results that we obtained for PEO-PBD copolymers and typical pictures are given in the ESI.† Giant polymersomes were only obtained for two of the polymers, namely PEO3900-PBD6700 and PEO1300-PBD2100, the first one yielding larger polymersomes. These corresponded to a very narrow PEO fraction of 0.37–0.38. Various conditions were evaluated, by changing the temperature and the applied voltage. Increasing the temperature from 30 °C to 70 °C led to a faster

process, polymersome formation being typically followed for 4 hours. At 70 °C however, degradation of polymersomes by bursting was observed at the end of the process. Increasing the voltage successively to 6, 9 and 12 V led to the inhibition of the formation process on the home-made device, but not on the commercial one. At 12 V, the surface degradation of ITO slides occurred in some cases. Thus, the optimal temperature and applied voltage were found to be 50 °C and 6 V.

The giant polymersomes were undamaged if resuspended in a solution of glucose of the same osmolarity. As a complement, we also examined the electroformation of poly(methyloxazoline-*b*-dimethylsiloxane-*b*-methyloxazoline) PMOXA1500-PDMS4500-PMOXA1500 polymersomes (corresponding to a hydrophilic fraction of 0.4). The same protocol was used (6, 9 or 12 V, 10 Hz, either 50 or 70 °C) and polymersomes were obtained for a 12 V voltage (a typical photograph is shown in the ESI†). To our knowledge, PMOXA-PDMS-PMOXA was known to lead to giant polymersomes but only one example had been described using electroformation.³³ It should be noted that the work presented here is focused on PEO and the results obtained are applicable only to polymers containing this hydrophilic block. Changing the hydrophilic block could change the self-assembly process by the modification of the interaction parameter with water.

Table 5 Results obtained from the "film rehydration" method

Polymers	$f_{\text{PEO exp}}$	DLS size int (nm)	DLS size number (nm)	PDI	Morphology from TEM
PEO5000-PCL33300	0.13	270	170	0.4	Polymersomes/NP ^a ?
PEO2000-PCL13300	0.13	410	110	0.6	Polymersomes/micelles/particles
PEO2000-PCL8800	0.19	100/400	90	0.7	Worm-like systems/polymersomes/micelles
PEO2000-PCL6700	0.23	250/30	30	0.9	Undefined shape NPs/polymersomes/worm-like systems
PEO2000-PCL5800	0.26	480/70	60	0.8	Micelles/aggregates ^a
PEO5000-PCL10800	0.31	500/20	20	1.0	Micelles/aggregates
PCL12300-PEO5000-PCL12300	0.17	150	150	0.9	Polymersomes/NP ^a ?
PEO3900-PBD6700	0.37	150/630	120/600	0.5	Worm-like systems, polymersomes

^a No TEM performed, morphology suggested only from DLS size.

Table 6 Formation of PEO-PBD polymersomes by electroformation under different conditions

PEO-PBD polymer	$f_{\text{PEO exp}}$	T ($^{\circ}\text{C}$)	Amplitude (peak to peak, V)	Observations by optical microscopy
3900–6700	0.37	30	6	None or small polymersomes
1300–2100	0.38			None
900–2300	0.28	50	6	None
2000–3800	0.34			None
3900–6700	0.37			Polymersomes $< 50 \mu\text{m}$
1300–2100	0.38			Polymersomes $< 10 \mu\text{m}$
1500–2300	0.39			None
3900–6700	0.37	70	6	Small polymersomes
1300–2100	0.38			Small polymersomes $< 8 \mu\text{m}$ in small quantities
3900–6700	0.37	50	9	None
2000–3800	0.34	50	12	None
3900–6700	0.37			None ^a or polymersomes $\geq 10 \mu\text{m}^b$
1500–2300	0.39			None
2000–3800	0.34	70	12	None
3900–6700	0.37			Polymersomes $\geq 24 \mu\text{m}^b$
1500–2300	0.39			None

^a On the home-made system. ^b On the Nanion device.

PCA analysis

In order to reveal the main structural or experimental factors that govern the formation of a specific family of self-assembly, a principal component analysis (PCA) was performed. A first PCA is presented in Fig. 3 which considers all samples for which a complete experimental dataset is available (*i.e.* size from DLS, TEM, SEC, ...). Each self-assembly system is defined by different variables: some of them related to structural factors (hydrophilic fraction, average molecular weight of the different block and of the whole polymer), and others related to experimental measured data (mean size from TEM, PDI, DLS size int or number). The first and second principal components described 40% and 28% of the initial variance.

Initial analysis of the results from correlation measurements (see Fig. S1 in the ESI[†]) between the different variables that could be involved in the self-assembly formation revealed a strong correlation between sizes obtained from TEM and DLS measurements, which proves that solution drying and staining for TEM did not modify the nano-objects. A less pronounced correlation between these sizes and the hydrophilic fraction was also calculated. However, there is no correlation between these sizes and any of the average molecular weights. In addition, the PDI of the size distribution was not significantly correlated with any other variable. The absence of strong correlation between measured sizes and structural parameters underlined the crucial role of preparation methods. The score plots revealed several features enabling differentiation between polymersomes and other structures (Fig. 3).

The different systems are separated along the second principal component primarily according to their average molecular weight. In this direction, there is no separation between polymersomes and micelle or nanoparticle systems. Along the first principal component, in contrast, a clustering between polymersomes and other self-assembly families is clearly seen. This axis

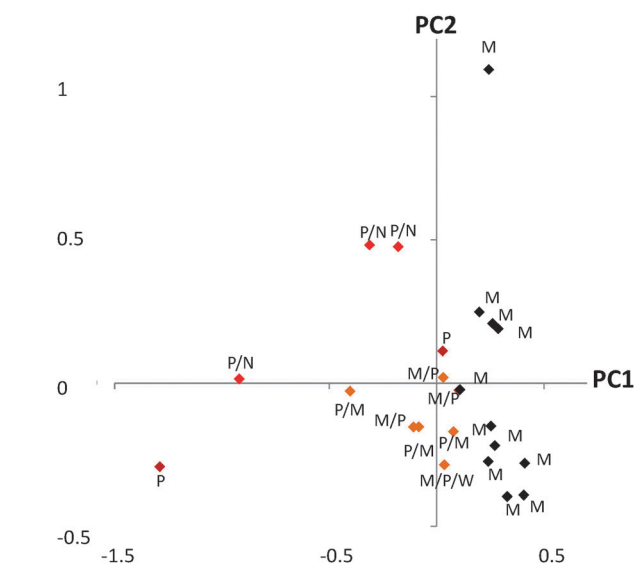


Fig. 3 PCA score plot from self-assemblies obtained by using different methods of formation from different families of block copolymers. The first principal component is positively correlated with the hydrophilic fraction and negatively correlated with size obtained from DLS or TEM whereas the second principal component is positively correlated with measured average molecular weights (from SEC or NMR) and PDI and negatively correlated with hydrophilic fraction (see the correlation plot in the ESI[†]). Morphologies were obtained from TEM. Legend: P: polymer-some, M: micelle, N: nanoparticle, and W: wormlike.

discriminates data mainly from the hydrophilic ratio (f_{PEO}) and the size measured from DLS and TEM analysis. It is also slightly correlated with the average molecular weight of the hydrophobic part but not with that of the hydrophilic part. Therefore, as expected and as stated in the subsequent discussion, f_{PEO} is the main structural parameter that favors the formation of polymersomes. In addition to using f_{PEO} , analyzing the size

through the PCA score plot allows us to discriminate polymersomes from other structures before performing further structural analyses such as cryo-TEM or multi-angle light scattering.

Discussion

Comparing our results with those of the literature will form the basis of our discussion to draw the reader's attention to delicate questions that scientists working on polymer self-assemblies have to deal with. The first point to keep in mind is the definition of polymersomes or polymer vesicles. If the word liposome is quite unambiguous for small surfactants, this is not as clear for polymers. One often expects that vesicles should have a large hydrophilic cavity in their core. This is the case for small surfactants, the only exception being to our knowledge vesicles formed from a polyoxometalate bolaform.³⁴ This is also the case for PEO-PBD polymersomes. However, in other objects that might still be classed as polymersomes because of the presence of an internal hydrophilic cavity, this might be quite small, as observed for PS-PAA vesicles.^{11,16,25} Indeed, the range of molecular weights of amphiphilic block copolymers is such that very different membrane thicknesses may be formed and the boundary between nanospheres and vesicles may not always be clear.⁷ While liposome membranes are typically 3–5 nm thick, those of polymer vesicles may vary between 3 and 50 nm.^{11,14,19,25}

Use of hydrophilic fraction for the prediction of self-assembly morphologies

The prediction of morphologies is linked to thermodynamic considerations, it is thus worthwhile to highlight specificities of polymers. The polymer assembly induces a chain entropy loss that can have a considerable effect on the resultant structure if a thermodynamic equilibrium is reached. Moreover, enthalpic factors related to the chemical structure are also involved through polymer–polymer and polymer–solvent interactions that play a critical role in assembly formation. Therefore the equilibrium morphology of block–copolymer aggregates depends on the stretching entropy of the chains in the core, the repulsions between the chains in the corona (both of which depend on the polymer/solvent interaction parameter) and the interfacial tension between the solvent and the core-forming block. Lastly, depending on the process used, kinetic phenomena may also be involved in the control of the final morphology. For instance the method used to switch from a good solvent to a poor one for a chosen block can greatly influence morphology. The example of PEO2000-PMMA5040 is the most spectacular, leading to 29 nm micelles when the assemblies are formed in the presence of acetone (Table 1) and to 550 nm polymersomes when they are formed by the slow addition of benzyl alcohol solution into THF/MeOH (Table 3). The final nano-objects are often frozen, *i.e.* not at thermodynamic equilibrium, and this limits the theoretical predictions. It is noteworthy that, to our knowledge, Pluronics are the only commercial polymers leading to thermodynamically controlled self-assemblies. Other examples exist in the literature, but they involve the introduction of hydrophilic moieties in the hydrophobic block.³⁵

Since the onset of polymersome studies, people have tried to establish simple rules that could be used to predict the self-assembly morphology of polymers, analogous to the packing parameter introduced by Israelachvili (see ESI†). Although this parameter is often mentioned when discussing polymer self-assemblies, it is not fully adequate to describe these owing to the particularities of polymer solution thermodynamics and kinetics mentioned above.

Table 7 presents self-assembly examples with an emphasis on polymersomes, from nanometric to giant (*i.e.* above 1 μm). This table is not exhaustive, but highlights some general and particular features that should be kept in mind when considering polymer self-assemblies. From a general standpoint, the most studied polymers are PEO-PBD, PEO-PEE, and PS-PAA polymers as well as amphiphilic polymers based on polyesters.

A few triblock polymers have also been examined, such as PEO-PPO-PEO or PEO-PLLA-PEO. Some polymers have been omitted from this table owing to the very limited number of studies performed on them.^{30,36–38} A general comment on this table is that the same trend of vesicles/worm-like systems/micelles is observed when increasing the hydrophilic fraction, even though the method of formation varied. The same comment is also valid in the case of our experiments, although clear delimited areas are not present.

Among these studies, early ones used the hydrophilic volume fraction f for comparing polymers, based on polymer solution thermodynamics models developed by Flory and Huggins. Later on, many authors used hydrophilic weight fractions for convenience. The equation used to switch between the weight and the volume fraction is given in the ESI.†

Discher and Eisenberg proposed in 2002¹⁶ the hydrophilic fraction as a parameter which could describe the block-copolymer asymmetry. By scanning polymer self-assemblies of PEO-PBD and PEO-PEE with molecular weights between 2700 and 20 000 g mol^{-1} , they observed that polymersomes were obtained for hydrophilic fractions f close to 0.35, micelles for $f > 0.45$ and inverted systems for $f < 0.25$. This rule has further evolved since then and currently the commonly accepted one is that micelles are obtained for hydrophilic fractions higher than 0.5, cylindrical systems for $0.4 < f < 0.5$ and vesicles for $f < 0.4$.^{3,39} The lower limit for vesicles remains unclear, however, with Discher mentioning a lower limit of 0.25³⁹ and Feijen one of 0.1.³ The suggested trend, with an existing order of morphologies going from vesicles to worm-like systems and finally micelles with increasing hydrophilic fractions, has been generally observed. However, not unexpectedly, the limit between each region is not always the same. As an example, PEO-PCL leads to vesicles for hydrophilic fractions typically between 0.1 and 0.3.³¹ The coexistence of several morphologies is frequently mentioned.^{25,29,31,40–42} In a very thorough paper,³¹ Therien demonstrated that for lower hydrophilic fractions, a new area of micelles may be found, together with particles. Our findings are in broad agreement with the comments above, as emphasized by the PCA analysis (Fig. 3). For most polymers, polymersomes are obtained for low hydrophilic fractions, but this cannot be used by itself to find a common threshold value.

Table 7 Examples of polymer self-assemblies

Polymer	$f_{\text{hydrophilic}}$ (weight fraction)	Self-assembly size (nm)	Morphology order appearance	Method of fabrication	Ref.
PEO-PEE	0.46	200–10 000	Polymersomes	Film rehydration, electroformation or direct dissolution	12 and 13
PEO-PBD	0.24–0.65	90–5000	Tubes/polymersomes/spheres	Film rehydration, electroformation	13, 14, 36, 41, 43 and 44
PS-PAA	0.01–0.15	20–1000	Micelles, polymersomes, rods	Cosolvent addition	11, 16 and 25
PEO-PPO-PEO	0.1	60–500	Vesicles	Direct dissolution or electroformation	44
	0.5–0.8		No vesicles		
PEO-PBO	0.32	130–15 000	Vesicles (?)	Film rehydration	28 and 45
PEO-PLLA	0.32–0.48	50	Vesicles	Direct dissolution or film rehydration	46
PEO-PDLLA	0.1–0.25	250–700	Vesicles	Cosolvent addition	24
PEO-PDLA/PEO-PLLA	0.3–0.7	30–60	Micelles (?)	Cosolvent addition	47
PEO-PLLA-PEO	0.2–0.57	20–100	Polymersomes/worm-like assemblies/micelles	Direct dialysis	42
PEO-PCL	0.07–0.33	100–5000	Micelles/polymersomes/micelles	Film rehydration or cosolvent addition	24, 30, 31 and 48–50
PEO-PMCL	0.24	100	Cylinders	Direct dissolution	29
	0.13–0.2		Vesicles		
PCL-PEO-PCL	0.2–0.6	100–300	Polymersomes/micelles	Cosolvent addition or film rehydration	51 and 52
PEO-PTMC	0.19	300	Vesicles	Cosolvent addition	24

PEO: poly(ethylene oxide), PEE: poly(ethylethylene), PBD: poly(butadiene), PS: polystyrene, PAA: poly(acrylic acid), PPO: poly(propylene oxide), PLLA: poly(L-lactide), PDLLA: poly(D,L-lactide), PLA: polylactide, PDLA: poly(D-lactide), PCL: poly(ϵ -caprolactone), PMCL: poly(γ -methyl ϵ -caprolactone), PTMC: poly(trimethylene carbonate), and PBO: poly(butylene oxide).

Since the use of the hydrophilic fraction as a universal parameter to predict the morphology of different block copolymers is controversial, several alternatives have been suggested. Rajagopal *et al.* recently introduced a modified hydrophilic parameter in the case of PEO-PCL self-assemblies where the contribution of the two oxygen atoms in the hydrophobic block units is taken into account.⁵³ In this way, the phase boundary between spherical micelles and the other morphologies is shifted to 0.5 similar to the case of PEO-PBD and PEO-PEE. Nevertheless, this hydrophilic parameter is considered too simplistic by some authors. Following the findings of Rajagopal *et al.*,⁵³ we calculated the modified hydrophilic fraction f_{hydr} (including oxygen atoms of the hydrophobic block into the hydrophilic part, see Table S2, ESI[†]). As in Discher's work, this led to a much higher vesicle-forming threshold (0.37 instead of 0.13) for PEO-PCL polymers. For PEO-PMMA, a similar evaluation was made and the absence of polymersomes could be explained by too high hydrophilic fraction (>0.42). However, in the case of PEO-PLA copolymers, the formation of either worm-like systems or vesicles was observed for f_{hydr} as high as 0.55, which does not fit with the simple rule suggested from PEO-PBD copolymers. A reduced tethered density of the hydrophilic block chains at the hydrophilic–hydrophobic interface has also been suggested.⁵⁴ The determination of this parameter is not straightforward, however, and can only be done *a posteriori* once the object dimensions are known.

The results presented in this work and the literature therefore stress that, while a tendency exists to form assemblies in a trend of vesicles/worm-like systems/micelles for increasing f_{PEO} , no common threshold can be recognized for different polymers, at least according to their hydrophilicity or related parameters.

Inherent polymer chain parameters

The analysis of our results shows different self-assembly behaviours. The differences observed between the various polymers

could be attributed to several parameters: different molar mass ranges (3000–70 000 g mol⁻¹), different glass transitions (see ESI[†]), or different crystallinities (PCL, PDLA and PLLA are semi-crystalline polymers). It is noteworthy that the PCA analysis performed here did not take into account glass transition temperature or crystallinity.

Regarding molar masses, as mentioned in Fig. 3, no correlation was observed between the molar mass of any block and the sizes of the nano-objects obtained. In other words, molar mass does not seem to be a critical parameter to determine morphology. Most often, in the literature, for PEO-PBD and PEO-PEE, the molar mass of the chains is less than 10 000 g mol⁻¹,^{12–15,36,43,44} which is different from the cases presented here. Higher molar masses have been reported in the literature, for instance for PS-PAA copolymers^{11,16,25,41} or PEO-polyesters.^{24,31,46,50} In the case of PS-PAA, Eisenberg suggested to denominate as “crew cut aggregates” the systems formed from copolymers having short hydrophilic blocks. For these, the same trend of micelles/worm-like systems/vesicles was observed, but at different hydrophilic fractions. However, these are not directly comparable since in the case of PS-PAA, polyelectrolyte properties might interfere with the formation of the self-assemblies, while in the case of polyesters, the method of fabrication is not the same.

Another possible parameter is the difference in glass transition temperature. This must be rejected since PEO-PBD and PEO-PEE exhibit a glass transition at around -4 °C and -30 °C, respectively. The polymers presented here exhibit glass transitions either below (PCL T_g at -62 °C) or above this range (PDLLA 50 °C, PMMA 105 °C, PS 95 °C). It is noteworthy that PEO5000-PCL4000 and PEO5000-PMMA4100 both led to micelles having the exactly same size, using the acetone cosolvent method, as determined by DLS (Table 1).

Finally, differences in semi-crystallinity are possible causes of different morphologies. This is most clearly seen in PEO-PDLA

and PEO-PLLA, where nanocrystals are obtained, whereas PEO-PDLLA always led to spherical morphologies. Discher and coworkers described the formation and the characterization of PEO-PCL assemblies by the cosolvent method using chloroform or film rehydration. They observed the same trend of micelles/worm-like systems/vesicles, and established that crystallization of PCL chains led to rigid vesicles, compared to PEO-PBD.⁵³ For this point, the case of polylactide polymers might also be instructive but unfortunately the number of publications on PLA-based vesicles is limited.²⁴

Other specific cases involve stereocomplexes^{47,55} or polyelectrolytes.^{11,16,25,41}

In all these cases, the addition of a cosolvent is necessary in order to form the nano-objects.¹⁶ Depending on the preparation protocol, kinetically frozen, non-equilibrium block-copolymer self-assemblies may be obtained and, as a consequence, not only the different steps of the preparative method, but also the solvent used influences the final morphology, which becomes almost impossible to predict.

Morphology determination

An important point to mention is the challenge of clearly assigning morphologies to the objects obtained. In this study, this has been mainly done by TEM analysis where small dense particles are described as micelles and larger particles as polymersomes or nanoparticles. Angular shapes were indicative of nanoparticles whereas round shapes could either be polymersomes or filled nanospheres. While this is sufficient for small objects (< 50 nm), it is no longer true for larger ones. Indeed, only a full characterization either by cryo-TEM,^{12,15,30,41,43,46,48} cryo-SEM, or dual static/dynamic light scattering^{29,50,51,56} allows the establishment of the internal morphology. The morphology determination is then based on the determination of the ratio between gyration and hydrodynamic radii. For homogeneous spheres, this ratio is expected to be 0.774, for empty spheres such as polymersomes with large cavities the value should approach 1 and may increase up to 2 for elongated objects depending on the anisotropy. However, for polymersomes having a small inner cavity, the value for R_g/R_h will obviously deviate from 1. For dual static/dynamic light scattering, the morphology may be determined only for objects in the range of 20–150 nm so that the scattered intensity is high enough and the explored q range is large enough to guarantee a correct analysis of the Guinier region. In some instances, SANS or SAXS are also used and data can be analyzed using adequate models, which often need many fitting parameters (like membrane thickness, polymersome radii and composition) and the analysis is complicated by the polydispersity arising from most formation processes. For this reason, these techniques are often coupled to microscopy observations in order to ensure a trustworthy picture of the system.^{29,43,44,47} For self-assemblies larger than 300 nm, these methods are no longer useful. For the giant polymersomes, direct observation of the self-assemblies by optical or fluorescence microscopy usually provides evidence of the vesicular structure.^{12–14,30,31,36,44,45,48} For intermediate range vesicles,

cryo-TEM or cryo-SEM can provide the answer. Fig. 2 presents examples of cryo-SEM pictures showing the presence of cavities.

Problem of self-assemblies' quantity

Depending on the formation technique and the polymer concentration, either large numbers of self-assemblies will be formed or only a few. The discrepancy is clearly visible comparing TEM images from cosolvent methods using either acetone, acetonitrile or THF/MeOH as the organic solvent, compared to Meng's method or film rehydration (see ESI†). When a large number of objects are formed, their characterization is easier and DLS and TEM are easy to compare. In contrast, great care should be taken for the interpretation of methods leading to a small number of self-assemblies. For DLS the level of scattered light received by the detector should always be checked to assess its difference compared to the background. A weak signal greatly impairs the size distribution then obtained, which should be taken with extreme caution as most routine algorithms are not adapted to extract values from this. Furthermore, one should always be aware of the possible presence of non-scattering or poorly scattering molecules or self-assemblies. Moreover since the scattered light is strongly dependent on the size of the scattering objects (see ESI† for details), large self-assemblies will always be overrepresented in the intensity-weighted apparent distribution. To avoid such biases, a fractionation technique such as Asymmetrical Flow Field Flow Fractionation has been shown to be very powerful.^{27,56} Using this technique, the presence of either free polymer or assemblies formed by only a few polymer chains can be distinguished and quantified compared to the largest nano-objects.

Influence of the formation method

A comparison of the results obtained in this study with the literature shows the importance of the preparation protocol when dealing with polymer self-assemblies. PEO-PCL and PEO-PLA will be particularly examined for this. Meng and Feijen in 2003 were among the first to describe polyester vesicles with the aim of forming artificial cells. They examined several methods using a cosolvent which could be either chloroform, THF, ethyl acetate or dioxane. The regular addition of chloroform led to large vesicles, but the subsequent removal of chloroform proved to be problematic. This is why they designed an original method of injecting the organic solution at the bottom of the aqueous phase without any stirring. In their case, the largest vesicles were obtained when a THF solution was added in this manner to a 4 wt% benzyl alcohol aqueous solution. They described the formation of 600 nm vesicles for PEO-PDLLA with f_{EO} of 0.1 and 0.2 and 450 nm ones for PEO-PCL with f_{EO} at 0.2.^{24,57} The closest cases in our study were those of PEO2000-PCL13300 ($f_{EO} = 0.13$) and PEO5000-PDLLA20500 ($f_{EO} = 0.2$). For the first one, 300 nm polymersomes were obtained while the latter yielded 130 nm polymersomes. Although leading to similar morphologies, both results are far apart in regard to the size from those described by Meng, and no clear interpretation for this can be given yet. One possibility could be in the kinetic control of the object formation such that even a small experimental

detail can be extremely important to get reproducible results. Later on, Hammer and Therien published the formation of PEO2000-PCL12000 ($f_{EO} = 0.14$) vesicles by a film rehydration method.⁴⁸ The vesicles were initially over 5 micrometers and could be reduced after extrusion to *ca.* 100 nm. PEO2000-PCL13300 in our case led to the formation of mixed morphologies of micelles, polymersomes and particles, none of which appeared to be larger than 1 μm . The higher polymer concentration in the initial solution and the slower vacuum evaporation in the work by Therien *et al.* could possibly explain the different results. In 2008, Stepanek and colleagues studied the formation of self-assemblies of PEO-PCL with hydrophilic fractions at 0.14, 0.28 and 0.5.^{49,50} In all cases, they obtained vesicles as evidenced by SLS and DLS characterizations. If this is in agreement with the behavior of PEO5000-PCL33300 studied here, the other cases are quite surprising compared to our results. Here again, although the trend is similar, the exact threshold for the different self-assemblies varies with the method. Indeed, the technique employed by Stepanek used THF as cosolvent in THF/water mixtures that were far from the large excess of water used here. Stepanek used a further dialysis step to decrease the organic solvent quantity upon several hours. This provides a further point worthy of discussion, *i.e.* the method of cosolvent elimination. In the experiments presented here, the cosolvent is either removed by simple evaporation or dialysis. Indeed, the formation method that is being discussed here has to be understood in its whole, meaning not only the cosolvent or film hydration method but also how the cosolvent is removed and over which period. The results presented here are therefore only valid for the exact preparation techniques described.

Finally Therien and Hammer recently published a thorough study of the micro- and nanoparticles formed for various PEO-PCL polymers.³¹ Both molar masses (from 3600 to 57 000 g mol^{-1}) and hydrophilic fractions (from 0.07 to 0.33) were varied. The technique used was film rehydration possibly followed by extrusion. They suggested that the different self-assemblies may be classified by cross-examining these parameters and proposed related graphs. These exhibited areas of single morphologies together with interpenetrated ones. They highlighted the difference in morphologies that could be observed between the micrometric scale and the nanometric one. Their results are however not directly comparable to ours, even regarding Table 5 dealing with film rehydration, because the nanometric morphologies in their case were characterized only after sonication, freeze-thaw extraction and extrusion.

Regarding the specific cases of giant polymersomes, some remarks can be made for the technique of electroformation. Comparing our results with the literature shows that differences are clearly obtained depending on the set-up, even though the polymers are supposed to be almost the same. Temperature variations between 50 and 70 $^{\circ}\text{C}$ are described in the literature, as well as varying field strengths, typically between 2 and 9 V.^{36,44,51,58} It is noteworthy that in our case, a 9 or 12 V potential led to the formation of polymersomes on the Nanion device whereas none were obtained on a home designed system. This highlights the problems of reproducibility from one set-up

to the other and the differences in film morphologies. Interestingly, the method of our study used the direct hydration of the film immediately followed by electroformation. In order to evaluate the fabrication method, we also performed the electroformation following a protocol described by Monroy where the dry polymer film is first subjected to an electric field before coupling hydration and electroformation.⁴⁴ Two polymers of Monroy's study are very close to the ones here, namely PEO3900-PBD6500 (OB3 in Monroy's article) and PEO1300-PBD2500 (OB2 in Monroy's article). Monroy described the formation of giant vesicles for OB2 but none for OB3. Here, following the same protocol, we observed polymersomes for PEO3900-PBD6700 but none for PEO1500-PBD2300. A different thickness of the film may explain such a difference. The quality of the polymer film is another essential experimental parameter that may explain differences. The chosen examples of this part emphasize once again the great caution that should be taken when addressing polymersome formation.

Conclusions

The results of this work in comparison with those of the literature show that one should be indeed very cautious when examining polymer self-assemblies: only a general trend of formation of objects is possible where micelles are preferably formed for high hydrophilic fractions f , followed by worm-like systems and vesicles when decreasing f . The threshold between the different morphologies not only depends on the chosen block-copolymer, but also on small details in the preparation method. The choice of solvent in the so-called cosolvent methods has been shown to influence not only the size but also possibly the morphology obtained. The order of addition of solvents has been observed to modify the size of the self-assemblies without changing the morphologies. An essential point to keep in mind is that polymer self-assemblies are very often formed out of thermodynamic equilibrium and are kinetically frozen systems, explaining the near impossibility of predicting their morphologies. Regarding the possible analysis of results however, PCA treatment was found to be a very useful tool to critically analyze the observed trends.

Acknowledgements

This work has been carried out in the framework of the ANR Poytransflow (13-BS09-0015). S. Balor (IBCG) is also acknowledged for cryo-TEM characterization.

Notes and references

- 1 K. Riehemann, S. W. Schneider, T. A. Luger, B. Godin, M. Ferrari and H. Fuchs, *Angew. Chem., Int. Ed.*, 2009, **48**, 872.
- 2 A. Gabizon, H. Shmeeda and T. Grenader, *Eur. J. Pharm. Sci.*, 2012, **45**, 388.
- 3 J. S. Lee and J. Feijen, *J. Controlled Release*, 2012, **161**, 473.

- 4 M. Yokoyama, M. Miyauchi, N. Yamada, T. Okano, Y. Sakurai and K. Kataoka, *Cancer Res.*, 1990, **50**, 1693.
- 5 Y. Bae, N. Nishiyama, S. Fukushima, H. Koyama, M. Yasuhiro and K. Kataoka, *Bioconjugate Chem.*, 2005, **16**, 122.
- 6 N. Nishiyama and K. Kataoka, *Pharmacol. Ther.*, 2006, **112**, 630.
- 7 K. Letchford and H. Burt, *Eur. J. Pharm. Biopharm.*, 2007, **65**, 259.
- 8 J. Shi, A. R. Votruba, O. C. Farokhzad and R. Langer, *Nano Lett.*, 2010, **10**, 3223.
- 9 A. Feng and J. Yuan, *Macromol. Rapid Commun.*, 2014, **35**, 767.
- 10 N. Bertrand and J. C. Leroux, *J. Controlled Release*, 2012, **161**, 152.
- 11 L. Zhang and A. Eisenberg, *Science*, 1995, **268**, 1728.
- 12 B. M. Discher, W. You-Yeon, D. S. Ege, J. C. M. Lee, F. S. Bates, D. E. Discher and D. A. Hammer, *Science*, 1999, **284**, 1143.
- 13 H. Aranda-Espinoza, H. Bermudez, F. S. Bates and D. E. Discher, *Phys. Rev. Lett.*, 2001, **87**, 208301.
- 14 J. C. M. Lee, H. Bermudez, B. M. Discher, M. A. Sheehan, Y.-Y. Won, F. S. Bates and D. E. Discher, *Biotechnol. Bioeng.*, 2001, **73**, 135.
- 15 H. Bermudez, A. K. Brannan, D. A. Hammer, F. S. Bates and D. E. Discher, *Macromolecules*, 2002, **35**, 8203.
- 16 D. E. Discher and A. Eisenberg, *Science*, 2002, **297**, 967.
- 17 P. J. Photos, L. Bacakova, B. Discher, F. S. Bates and D. E. Discher, *J. Controlled Release*, 2003, **90**, 323.
- 18 R. Dimova, U. Seifert, B. Pouligny, S. Förster and H.-G. Döbereiner, *Eur. Phys. J. E: Soft Matter Biol. Phys.*, 2002, **7**, 241.
- 19 J.-F. Le Meins, O. Sandre and S. Lecommandoux, *Eur. Phys. J. E: Soft Matter Biol. Phys.*, 2011, **34**, 14.
- 20 F. Meng, Z. Zhong and J. Feijen, *Biomacromolecules*, 2009, **10**, 197.
- 21 K. Knop, A.-F. Mingotaud, N. El-Akra, F. Violleau and J.-P. Souchard, *Photochem. Photobiol. Sci.*, 2009, **8**, 396.
- 22 C. Sanson, C. Schatz, J.-F. O. Le Meins, A. Brûlet, A. Soum and S. B. Lecommandoux, *Langmuir*, 2010, **26**, 2751.
- 23 L. Gibot, A. Lemelle, U. Till, B. Moukarzel, A. F. Mingotaud, V. Pimienta, P. Saint-Aguet, M. P. Rols, M. Gaucher, F. Violleau, C. Chassenieux and P. Vicendo, *Biomacromolecules*, 2014, **15**, 1443.
- 24 F. Meng, PhD thesis, University of Twente, 2003.
- 25 O. Terreau, C. Bartels and A. Eisenberg, *Langmuir*, 2004, **20**, 637.
- 26 D. J. Adams, C. Kitchen, S. Adams, S. Fuzeland, D. Atkins, P. Schuetz, C. M. Fernyhough, N. Tzokova, A. J. Ryan and M. F. Butler, *Soft Matter*, 2009, **5**, 3086.
- 27 J. Ehrhart, A.-F. Mingotaud and F. Violleau, *J. Chromatogr. A*, 2011, **1218**, 4249.
- 28 A. J. Parnell, N. Tzokova, P. D. Topham, D. J. Adams, S. Adams, C. M. Fernyhough, A. J. Ryan and R. A. L. Jones, *Faraday Discuss.*, 2009, **143**, 29.
- 29 J. Braun, N. Bruns, T. Pfohl and W. Meier, *Macromol. Chem. Phys.*, 2011, **212**, 1245.
- 30 J. S. Katz, K. A. Eisenbrown, E. D. Johnston, N. P. Kamat, J. Rawson, M. J. Therien, J. A. Burdick and D. A. Hammer, *Soft Matter*, 2012, **8**, 10853.
- 31 W. Qi, P. P. Ghoroghchian, G. Li, D. A. Hammer and M. J. Therien, *Nanoscale*, 2013, **5**, 10908.
- 32 M. I. Angelova, S. Soléau, P. Méléard, J. F. Faucon and P. Bothorel, *Prog. Colloid Polym. Sci.*, 1992, **89**, 127.
- 33 L. Theogarajan, S. Desai, M. Baldo and C. Scholz, *Polym. Int.*, 2008, **57**, 660.
- 34 S. Landsmall, M. Luka and S. Polarz, *Nat. Commun.*, 2012, **3**, DOI: 10.1038/ncomms2321.
- 35 D. B. Wright, J. P. Patterson, A. Pitto-Barry, P. Cotanda, C. Chassenieux, O. Colombani and R. K. O'Reilly, *Polym. Chem.*, 2015, **6**, 2761.
- 36 E. Mabrouk, S. Bonneau, L. Jia, D. Cuvelier, M.-H. Li and P. Nasso, *Soft Matter*, 2010, **6**, 4863.
- 37 J. J. L. M. Cornelissen, M. Fischer, N. A. J. M. Sommerdijk and J. M. N. Roeland, *Science*, 1998, **280**, 1427.
- 38 E. Mabrouk, D. Cuvelier, F. Brochard-Wyart, P. Nasso and M.-H. Li, *Proc. Natl. Acad. Sci. U. S. A.*, 2009, **106**, 7294.
- 39 D. A. Christian, S. Cai, D. M. Bowen, Y. Kim, J. D. Pajerowski and D. E. Discher, *Eur. J. Pharm. Biopharm.*, 2009, **71**, 463.
- 40 M. Antonietti and S. Förster, *Adv. Mater.*, 2003, **15**, 1323.
- 41 S. Jain and F. S. Bates, *Science*, 2003, **300**, 460.
- 42 X. Wu, S. Li, F. Coumes, V. Darcos, J. Lai Kee Him and P. Bron, *Nanoscale*, 2013, **5**, 9010.
- 43 W. You-Yeon, H. T. Davis and F. S. Bates, *Science*, 1999, **283**, 960.
- 44 R. Rodriguez-Garcia, M. Mell, I. Lopez-Montero, J. Netzel, T. Hellweg and F. Monroy, *Soft Matter*, 2011, **7**, 1532.
- 45 J. R. Howse, R. A. L. Jones, G. Battaglia, R. E. Ducker, G. J. Leggett and A. J. Ryan, *Nat. Mater.*, 2009, **8**, 507.
- 46 F. Ahmed and D. E. Discher, *J. Controlled Release*, 2004, **96**, 37.
- 47 N. Kang, M.-E. Perron, R. E. Prud'homme, Y. Zhang, G. Gaucher and J. C. Leroux, *Nano Lett.*, 2005, **5**, 315.
- 48 P. P. Ghoroghchian, G. Li, D. H. Levine, K. P. Davis, F. S. Bates, D. A. Hammer and M. J. Therien, *Macromolecules*, 2006, **39**, 1673.
- 49 R. Šachl, M. Štěpánek, K. Procházka, J. Humpolíčková and M. Hof, *Langmuir*, 2008, **24**, 288.
- 50 R. Sachl, M. Uchman, P. Matejicek, K. Procházka, M. Stepanek and M. Spirkova, *Langmuir*, 2007, **23**, 3395.
- 51 Y. Zhao, H. Liang, S. Wang and C. Wu, *J. Phys. Chem. B*, 2001, **105**, 848.
- 52 L. Zhang, Y. He, G. Ma, C. Song and H. Sun, *Nanomedicine*, 2012, **8**, 925.
- 53 K. Rajagopal, A. Mahmud, D. A. Christian, J. D. Pajerowski, A. E. X. Brown, S. M. Loverde and D. E. Discher, *Macromolecules*, 2010, **43**, 9736.
- 54 Z.-X. Du, J.-T. Xu and Z.-Q. Fan, *Macromolecules*, 2007, **40**, 7633.
- 55 F. K. Wolf, A. M. Hofmann and H. Frey, *Macromolecules*, 2010, **43**, 3314.
- 56 U. Till, M. Gaucher-Delmas, P. Saint-Aguet, G. Hamon, J.-D. Marty, C. Chassenieux, B. Payré, D. Goudounèche, A. F. Mingotaud and F. Violleau, *Anal. Bioanal. Chem.*, 2014, **406**, 7841.
- 57 F. Meng, G. H. M. Engbers and J. Feijen, *J. Controlled Release*, 2005, **101**, 187.
- 58 M. Chemin, P.-M. Brun, S. Lecommandoux, O. Sandre and J.-F. Le Meins, *Soft Matter*, 2012, **8**, 2867.